

Electron drift velocity in argon, nitrogen, hydrogen, oxygen and ammonia in strong electric fields determined from rf breakdown curves

V Lisovskiy^{1,3}, J-P Booth¹, K Landry², D Douai², V Cassagne² and V Yegorenkov³

¹ Laboratoire de Physique et Technologie des Plasmas, Ecole Polytechnique, Palaiseau 91128, France

² Unaxis Displays Division France SAS, 5, Rue Leon Blum, Palaiseau 91120, France

³ Kharkov National University, Kharkov 61077, Ukraine

E-mail: lisovskiy@yahoo.com

Received 27 September 2005, in final form 19 December 2005

Published 3 February 2006

Online at stacks.iop.org/JPhysD/39/660

Abstract

We report measurements of the breakdown curves for low-pressure rf capacitive discharges in nitrogen, hydrogen, argon, oxygen and ammonia. The electron drift velocity in these gases was deduced, as a function of reduced electric field, from the low-pressure turning points of the breakdown curves. The equation for rf breakdown proposed by Kihara (1952 *Rev. Mod. Phys.* **24** 52) allows the position of both the turning point and the breakdown curve minimum to be calculated from the transport properties of each gas. Therefore we propose a new technique to determine the electron drift velocity from the position of the rf breakdown curve minima. We have determined the drift velocity in the range $E/p = 52\text{--}1324\text{ V cm}^{-1}\text{ Torr}^{-1}$ for nitrogen, $E/p = 33\text{--}720\text{ V cm}^{-1}\text{ Torr}^{-1}$ for argon, $E/p = 32\text{--}713\text{ V cm}^{-1}\text{ Torr}^{-1}$ for ammonia, $E/p = 32\text{--}550\text{ V cm}^{-1}\text{ Torr}^{-1}$ for hydrogen and $E/p = 69\text{--}1673\text{ V cm}^{-1}\text{ Torr}^{-1}$ for oxygen.

1. Introduction

The electron drift velocity in an electric field, V_{dr} , characterizes the conductivity of a weakly ionized gas and is one of the most important electron transport parameters. There are a number of techniques (the time-of-flight technique, observation of the optical radiation of a moving electron swarm, the shutter technique and so on) that have been used to measure the electron drift velocity. However, they only work for comparatively small reduced fields, E/p , because at higher values a self-sustaining discharge is ignited which impedes the measurement. The authors of papers [1–4] have proposed a novel method for determining the electron drift velocity from the location of the turning point (where $dU_{\text{rf}}(p)/dp \rightarrow \infty$) in the low-pressure region of breakdown curves $U_{\text{rf}}(p)$ (U_{rf} is the amplitude of the rf voltage, p is the gas pressure) of rf capacitive discharges. Whereas conventional techniques become inapplicable after the ignition

of the self-sustaining discharge (i.e. for high reduced fields), this method is actually based on discharge ignition, allowing measurements of V_{dr} in strong electric fields. Recently we used this technique to determine the electron drift velocity in ammonia [5].

In this paper we have determined the electron drift velocity in nitrogen, hydrogen, argon, oxygen and ammonia using the same technique. We also have analysed the rf breakdown equation in order to find the positions of both the turning point and breakdown minimum. We propose a new technique for determining the electron drift velocity from the pressure and voltage coordinates of the rf breakdown curve minima. In this way we have deduced the drift velocity in the range $E/p = 52\text{--}1324\text{ V cm}^{-1}\text{ Torr}^{-1}$ for nitrogen, $E/p = 33\text{--}720\text{ V cm}^{-1}\text{ Torr}^{-1}$ for argon, $E/p = 32\text{--}713\text{ V cm}^{-1}\text{ Torr}^{-1}$ for ammonia, $E/p = 32\text{--}550\text{ V cm}^{-1}\text{ Torr}^{-1}$ for hydrogen and $E/p = 69\text{--}1673\text{ V cm}^{-1}\text{ Torr}^{-1}$ for oxygen.

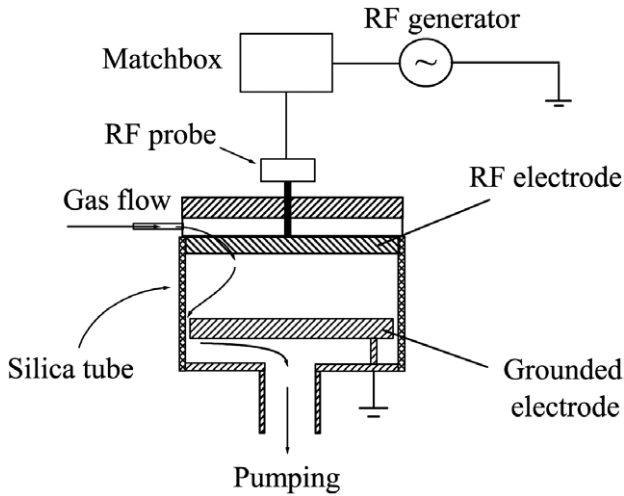


Figure 1. Schematic of the experimental setup.

2. Experimental setup

The rf discharge was ignited in the pressure range $p \approx 0.01\text{--}30$ Torr with rf frequencies of either $f = 13.56$ MHz or $f = 27.12$ MHz. The distance between the parallel-plate electrodes (143 mm in diameter) was varied over the range $L = 3\text{--}27$ mm. The rf voltage, with an amplitude $U_{\text{rf}} < 2000$ V, was fed to the upper electrode; the other one was grounded. The electrodes were located inside a fused silica tube with an inner diameter of 145 mm (see figure 1). The gas was supplied through small orifices in the powered electrode and then pumped out via the gap (1 mm) between the second electrode and the wall of the fused silica tube. This distance was necessary both to allow adequate gas flow and to allow for thermal expansion of the electrode, whilst preventing discharge ignition in this region.

The gas pressure was monitored with 1 and 10 Torr capacitive manometers (MKS Instruments). The gas flow was set with a mass flow controller to 5 sccm and the pressure regulated by throttling the outlet to the pump. The rf voltage was measured with an rf current–voltage probe (Advanced Energy Z’SCAN).

We used the technique proposed by Levitskii [6] to measure the breakdown curves of the rf discharge. Near to, and to the high-pressure side of, the breakdown curve minimum the gas pressure was fixed before slowly increasing the rf voltage until gas breakdown occurs. To the low-pressure side of the minimum the curve may be multi-valued, i.e. the curve turns back towards high-pressure and breakdown occurs at two different values of the rf voltage. Therefore in this range we first decreased the gas pressure, then fixed the rf voltage value and only then increased the gas pressure slowly until discharge ignition occurred. At the moment of discharge ignition the rf voltage shows a sharp decrease, and a glow appears between the electrodes serving as our criterion for the onset of gas breakdown. The uncertainty in the measured breakdown voltages did not exceed 1–2 V over the whole U_{rf} range under study.

3. Analysis of the electron motion in an electric field and of rf breakdown curves

Consider the motion of electrons in a uniform rf electric field in the collisional regime ($\nu_{\text{en}} \gg \omega$, where ν_{en} is the collision rate between electrons and gas molecules and $\omega = 2\pi f$ is the angular frequency of the rf field). The time-dependent electron drift velocity, $V_{\text{dr}}(t)$, is given by

$$V_{\text{dr}}(t) = \frac{eE_{\text{rf}}}{m\nu_{\text{en}}} \cos(\omega t), \quad (1)$$

where e and m are the electron charge and mass, respectively, and E_{rf} is the rf field amplitude. The maximum instantaneous drift velocity of electrons, V_{dr} , corresponding to the electron drift velocity at the rf field maximum is given by

$$V_{\text{dr}} = \frac{eE_{\text{rf}}}{m\nu_{\text{en}}}. \quad (2)$$

On integrating (1) over time we get the amplitude, A , of the electron displacement:

$$A = \frac{eE_{\text{rf}}}{m\nu_{\text{en}}\omega} = \frac{V_{\text{dr}}}{\omega}. \quad (3)$$

Kihara [7] derived the following criterion for gas breakdown in a uniform rf electric field:

$$\frac{\nu_i}{D_e} = \frac{1}{\Lambda^2} = \frac{\pi^2}{(L - 2A)^2} = \frac{\pi^2}{(L - 2(V_{\text{dr}}/\omega))^2}, \quad (4)$$

where ν_i is the ionization rate of gas molecules via electron impact, D_e is the electron diffusion coefficient and Λ is the diffusion length. The ionization rate is related to the drift velocity by the Townsend coefficient, α : $\nu_i = \alpha \cdot V_{\text{dr}}$, where

$$\alpha = A_1 \cdot p \cdot \exp\left(-\frac{B}{E_{\text{eff}}/p}\right) \quad (5)$$

and E_{eff} is the effective electric field strength, $E_{\text{eff}} = E_{\text{rf}}/\sqrt{2}$, A_1 and B are constants depending on the gas species, $V_{\text{dr}} = \mu_e \cdot E = \mu_{e0} \cdot E/p$, $D_e = D_{e0}/p$, and μ_{e0} and D_{e0} are the electron mobility and diffusion coefficient at the gas pressure of $p = 1$ Torr, respectively. Inserting the expressions for ν_i , α , V_{dr} and D_e into equation (4) and rearranging gives the equation

$$\exp\left(\frac{\sqrt{2}BpL}{U_{\text{rf}}}\right) = A_1 \cdot p^2 \cdot \frac{\mu_{e0}}{D_{e0}} \cdot \frac{U_{\text{rf}}}{pL} \times \frac{(L - 2 \cdot (\mu_{e0}/\omega) \cdot (U_{\text{rf}}/pL))^2}{\pi^2}. \quad (6)$$

Here $U_{\text{rf}} = U_{\text{rf}}(p)$ is the amplitude of the rf voltage at breakdown. Now let us examine the derivative of the breakdown voltage with respect to the gas pressure, $dU_{\text{rf}}(p)/dp$. The rf breakdown curve minimum occurs when $dU_{\text{rf}}(p)/dp = 0$, and the turning point occurs when $dU_{\text{rf}}(p)/dp \rightarrow \infty$. Rather than presenting the cumbersome expression for $dU_{\text{rf}}(p)/dp$ we will simply give the results obtained for the two conditions given above. For the turning point (at U_t and p_t) we obtain the expression

$$U_t = \frac{1}{2} \cdot p_t L^2 \cdot \frac{\omega}{\mu_{e0}}, \quad (7)$$

$$\left(\frac{E}{p}\right)_t = \frac{U_t}{p_t L} = \frac{1}{2} \cdot L \cdot \frac{\omega}{\mu_{e0}}. \quad (8)$$

Inserting (8) into (3) gives

$$A = \frac{V_{dr}}{\omega} = \frac{\mu_{e0}}{\omega} \left(\frac{E}{p}\right)_t = \frac{L}{2}. \quad (9)$$

Hence the electron drift velocity, V_{dr} , at the turning point of the rf breakdown curve is equal to

$$V_{dr} = \frac{\omega \cdot L}{2} = L\pi f. \quad (10)$$

Equation (10) has been derived in previous papers [1–5]. In these papers it was assumed that at the turning point the amplitude of the electron displacement is equal to $A \approx L/2$. Prior to this Levitskii [6] had already proposed that the amplitude of electron displacement at the turning point would be approximately equal to the half-width of the inter-electrode distance; however none of the previous papers gave a rigorous proof of this assumption. Using Kihara's gas breakdown equation we have proved that at the turning point of the rf breakdown curve $A = L/2$. Thus the technique for determining the electron drift velocity from the turning point coordinates [1–5] is justified.

So at the turning point of the breakdown curve (corresponding to $p = p_t$ and $U_{rf} = U_t$) the amplitude of the electron displacement is equal to half of the gap: $A = L/2$. We can understand this in the following way: when the electron oscillation becomes larger than half the electrode spacing, the electron loss rate tends to infinity, making breakdown impossible, hence defining the lowest pressure at which breakdown can occur for the diffusion–drift branch. It follows from equation (10) that the value of the electron drift velocity at the turning point of the breakdown curve depends only on the values of the inter-electrode gap and the frequency of the rf field. At the same time it is independent of the gas species. Obviously, the electron drift velocity depends on the ratio of the electric field strength magnitude to the gas pressure E/p , and this dependence is different for different gases. But at the specific conditions (L, p, ω) corresponding to the turning point for any particular gas the amplitude of electron oscillations is equal to $A = L/2 = V_{dr}/\omega$ and the electrons will have the same drift velocity ($V_{dr} = L\omega/2$). However, the corresponding value of E/p at this point will be different for each gas. The coordinates of the turning point permit us to determine the reduced field, E/p , corresponding to this electron drift velocity.

At the breakdown curve minimum (with the coordinates U_{min} and p_{min}) the following expression is obtained:

$$U_{min} = \frac{\sqrt{2} p_{min} \cdot L}{8\mu_{e0}} \cdot \left(-4\mu_{e0} B - \sqrt{2} L \omega + \sqrt{16\mu_{e0}^2 B^2 + 24\sqrt{2}\mu_{e0} B \omega L + 2\omega^2 L^2} \right). \quad (11)$$

Solving for the electron mobility, μ_{e0} ,

$$\mu_{e0} = \frac{1}{2} \cdot p_{min} \cdot L^2 \cdot \omega \cdot \frac{2 \cdot B \cdot p_{min} \cdot L - U_{min} \cdot \sqrt{2}}{U_{min} \cdot (2 \cdot B \cdot p_{min} \cdot L + U_{min} \cdot \sqrt{2})}. \quad (12)$$

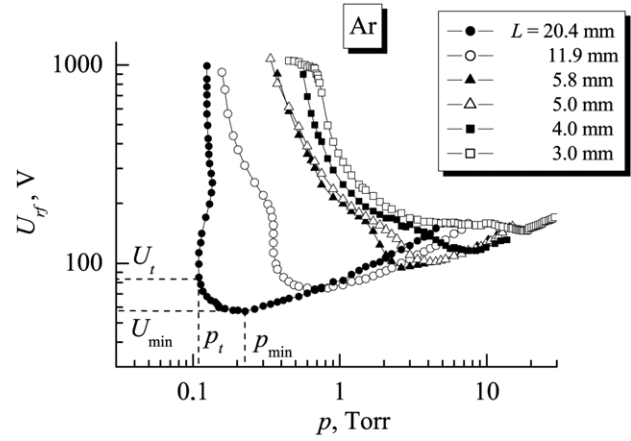


Figure 2. Rf discharge breakdown curves in argon for different inter-electrode gap values, $f = 13.56$ MHz, showing the location of a turning point, p_t and U_t , and the minimum, p_{min} and U_{min} , for the $L = 20.4$ mm curve.

From this we can obtain an expression for the electron drift velocity at the rf breakdown curve minimum:

$$V_{dr} = \mu_{e0} \cdot \left(\frac{E}{p}\right)_{min} = \mu_{e0} \cdot \frac{U_{min}}{p_{min} \cdot L} = \frac{\omega L}{2} \cdot \frac{2 \cdot B \cdot p_{min} \cdot L - U_{min} \cdot \sqrt{2}}{2 \cdot B \cdot p_{min} \cdot L + U_{min} \cdot \sqrt{2}}, \quad (13)$$

$$V_{dr} = \frac{\omega L}{2} \cdot \frac{B - (1/\sqrt{2})(E/p)_{min}}{B + (1/\sqrt{2})(E/p)_{min}}. \quad (14)$$

Thus we can also determine the electron drift velocity from the measured coordinates of the rf breakdown curve minimum. A disadvantage of this technique is that it depends on knowledge of the first Townsend coefficient α (because the constant B enters expressions (13) and (14)); therefore this technique can only be applied to the gases for which this first Townsend coefficient is already known. However, this new technique enables the electron drift velocity to be determined from rf breakdown curves which show no turning point.

4. Experimental results

The coordinates of the turning point allow the reduced field, E/p , to be determined for a known electron drift velocity. For example, let us take the coordinates of the turning point observed in the breakdown curve for argon with a gap of 20.4 mm at an rf frequency of 13.56 MHz (see figure 2): $p_t = 0.11$ Torr and $U_t = 84.8$ V. Then from formulae (8) and (10) it follows that $E/p = 529.1$ V cm⁻¹ Torr⁻¹ and $V_{dr} = 8.69 \times 10^7$ cm s⁻¹. Now let us take the coordinates of the minimum of the same breakdown curve: $p_{min} = 0.226$ Torr and $U_{min} = 57.2$ V. According to formulae (13) and (14) we get $E/p = 124.1$ V cm⁻¹ Torr⁻¹ and $V_{dr} = 3.0 \times 10^7$ cm s⁻¹. Thus the measured breakdown curve for one gap value provides two values of the electron drift velocity (provided that the breakdown curve possesses a diffusion–drift branch with a well-expressed turning point).

However, it is clear from figure 2 that the breakdown curves in argon for narrow gaps between the electrodes ($L < 1$ cm) have no turning point (under these conditions the

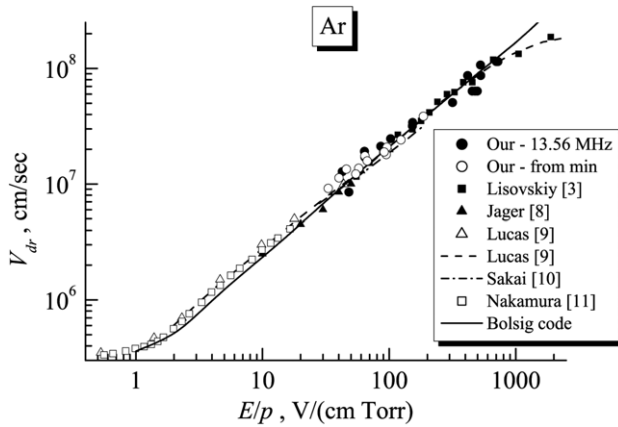


Figure 3. Electron drift velocity in argon against E/p . The solid curve presents the calculated data obtained with the Bolsig code, solid circles are our experimental data from turning points, empty circles are our experimental data from minima, solid squares are for the experimental data from [3], solid triangles are for the measured data from [8], empty triangles are for the experimental data from [9], dash curve presents the calculation data from [9], dash-dot curve presents the calculation data from [10] and empty squares are for the experimental data from [11].

diffusion–drift branch transforms smoothly into the Paschen branch without a multi-valued region or turning point). Consequently, we cannot determine the electron drift velocity from the coordinates of the turning point. However, these curves possess a well-expressed minimum which can be used instead to determine V_{dr} with our new technique. Therefore, when an rf breakdown curve possesses no turning point, we can determine only one value of the electron drift velocity from each breakdown curve. In order to obtain a set of V_{dr} values over a wide range of E/p , rf breakdown curves must be recorded at various values of the inter-electrode gap, L .

The values of the electron drift velocity in argon in the range $E/p = 33\text{--}720\text{ V cm}^{-1}\text{ Torr}^{-1}$ determined from our measured breakdown curves are presented in figure 3. The same figure shows previous measurements in the literature [3, 8–11]. The figure shows that our values, obtained from both the turning points and from the new technique using the breakdown curve minima, are in good agreement with the experimental and calculated values given by other authors.

Recently we published values of the electron drift velocity in ammonia obtained from the turning points of rf breakdown curves [5]. Figure 4 shows breakdown curves in ammonia at a frequency of 13.56 MHz, and figure 5 shows the electron drift velocities obtained from this data using the new ‘minima’ technique for the range $E/p = 32\text{--}713\text{ V cm}^{-1}\text{ Torr}^{-1}$. Our new results are in good agreement with the measured values in [5], along with values calculated with the Bolsig code (www.siglo-kinema.com/bolsig.htm). Bolsig is a code for the numerical solution of the Boltzmann equation for electrons in weakly ionized gases and in steady-state, uniform fields. This code was designed to generate electron and transport data in pure gases or gas mixtures over a wide range of values of E/p . Figure 5 also shows the experimental data obtained by the authors of papers [12–14]. However it is impossible to compare our results with theirs, as they only give values for very low ($E/p < 20\text{ V cm}^{-1}\text{ Torr}^{-1}$) reduced fields.

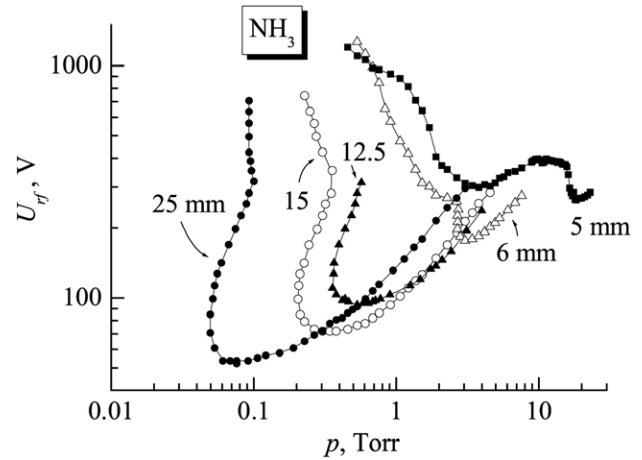


Figure 4. Rf discharge breakdown curves in ammonia for different inter-electrode gap values, $f = 13.56\text{ MHz}$.

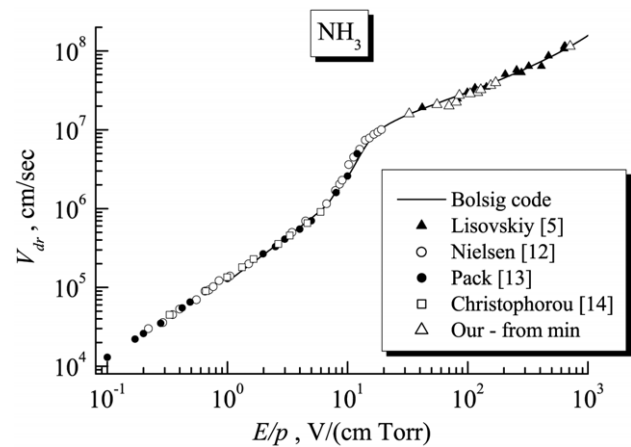


Figure 5. Electron drift velocity in ammonia against E/p . The solid curve presents the calculated data obtained with the Bolsig code, solid triangles are for the experimental data from [5], empty triangles are for our measured data, empty circles are for the experimental data from [12], solid circles are for the experimental data from [13] and empty squares are for the experimental data from [14].

Figure 6 shows measured rf breakdown curves in oxygen at 13.56 MHz. From these curves we derived the electron drift velocity over the range, $E/p = 69\text{--}1673\text{ V cm}^{-1}\text{ Torr}^{-1}$, shown in figure 7. The same figure shows the findings of papers [15–21, 27], which are in good agreement with our results.

Figure 8 presents measured breakdown curves in nitrogen for different values of the inter-electrode gap, L , and for two values of the rf field frequency: 13.56 and 27.12 MHz. For a fixed inter-electrode gap, L , the multi-valued region of the curves (observed to the left of the minimum of the diffusion–drift branch) is more pronounced at higher frequency. Therefore the technique based on the use of turning points should give more accurate results when a higher rf field frequency is used. Secondly, the right-hand branches of the breakdown curves recorded for a fixed gap, L , but for different frequencies, coincide at higher gas pressure. This feature is in agreement with the results obtained by Githens [22] and Chenot [23], who studied rf discharges over a broad range of rf

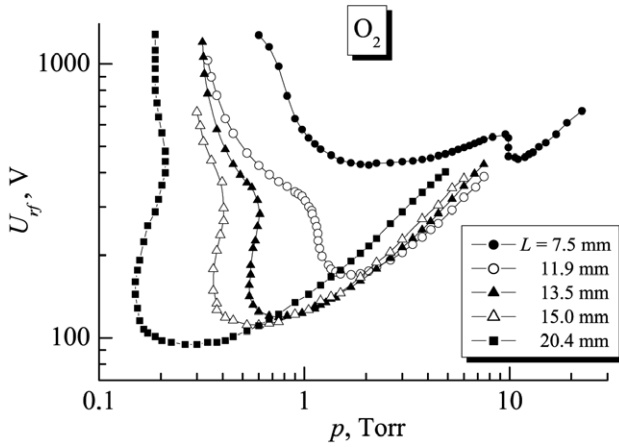


Figure 6. Rf discharge breakdown curves in oxygen for different inter-electrode gap values, $f = 13.56$ MHz.

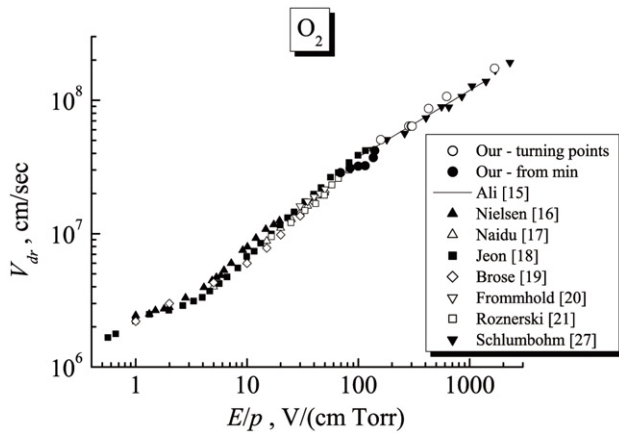


Figure 7. Electron drift velocity in oxygen against E/p . The empty circles are our experimental data from turning points, the solid circles are our experimental data from minima, the solid curve presents calculated data from [15], solid triangles are for the measured data from [16], empty triangles are for the experimental data from [17], solid squares are for the experimental data from [18], empty diamonds are for the experimental data from [19], empty upside-down triangles are for the measured data from [20], empty squares are for the experimental data from [21] and solid upside-down triangles are for the measured data from [27].

frequencies. Figure 9 presents values of the drift velocity for nitrogen gas over the range $E/p = 52\text{--}1324 \text{ V cm}^{-1} \text{ Torr}^{-1}$; the results obtained from the turning point for 13.56 and 27.12 MHz as well as from the breakdown curve minima (for the frequencies 13.56 and 27.12 MHz together) are shown separately. There is good agreement between our results (obtained using the different methods and frequencies) and those of previous publications [21, 25–30]. Figure 9 also shows values calculated using the Bolsig code and published cross-sections [31] for elastic as well as inelastic collisions between electrons and nitrogen molecules. The calculations are in good agreement with the experimental data (ours as well as by other authors).

Similar breakdown curves for rf discharges in hydrogen obtained for the frequencies of 13.56 and 27.12 MHz and for different inter-electrode gap values are shown in figure 10. From these curves we determined the electron drift velocity

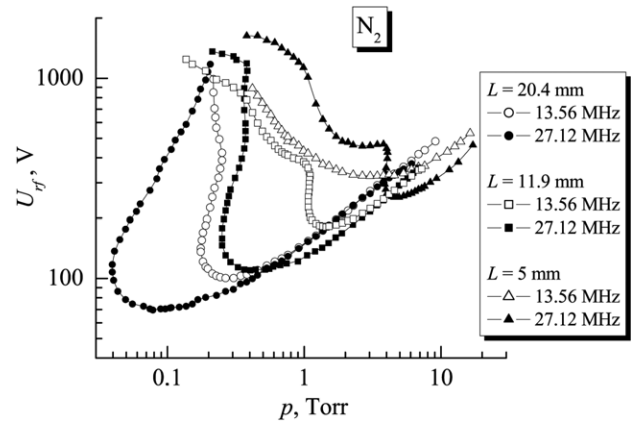


Figure 8. Rf discharge breakdown curves in nitrogen for different inter-electrode gap values and $f = 13.56$ MHz and $f = 27.12$ MHz.

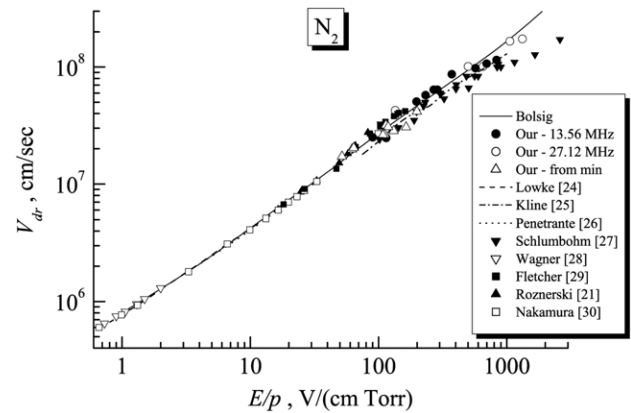


Figure 9. Electron drift velocity in nitrogen against E/p . The solid curve presents the calculated data obtained with the Bolsig code, the dashed curve presents the calculated data from [24], the dash-dot curve presents the calculated data from [25] and the dotted curve presents the calculated data from [26]. The solid circles are our experimental data from turning points ($f = 13.56$ MHz), the empty circles are our experimental data from turning points ($f = 27.12$ MHz), the empty triangles are our experimental data from minima ($f = 13.56$ MHz and $f = 27.12$ MHz), the solid upside-down triangles are for the measured data from [27], the empty upside-down triangles are for the experimental data from [28], the solid squares are for the experimental data from [29], the solid upright triangles are for the measured data from [21] and the empty squares are for the experimental data from [30].

over the range, $E/p = 32\text{--}550 \text{ V cm}^{-1} \text{ Torr}^{-1}$, presented in figure 11. These values are in good agreement with previous papers [3, 21, 24, 27, 32–34].

5. Conclusions

In this paper we have presented measured rf breakdown curves for rf frequencies of 13.56 and 27.12 MHz, and an analysis of Kihara's rf breakdown equation. We have determined the electron drift velocity in nitrogen, hydrogen, argon, oxygen and ammonia from the turning point of the breakdown curves of an rf capacitive discharge. We have proposed a new technique for determining the electron drift velocity from the coordinates of the rf breakdown curve minima. We have obtained the values of the electron drift

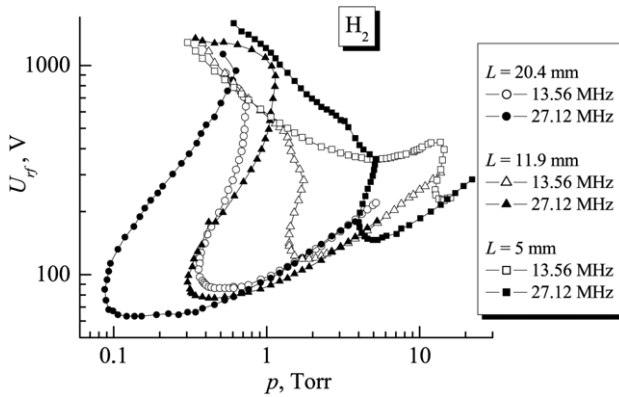


Figure 10. RF discharge breakdown curves in hydrogen for different inter-electrode gap values and $f = 13.56$ MHz and $f = 27.12$ MHz.

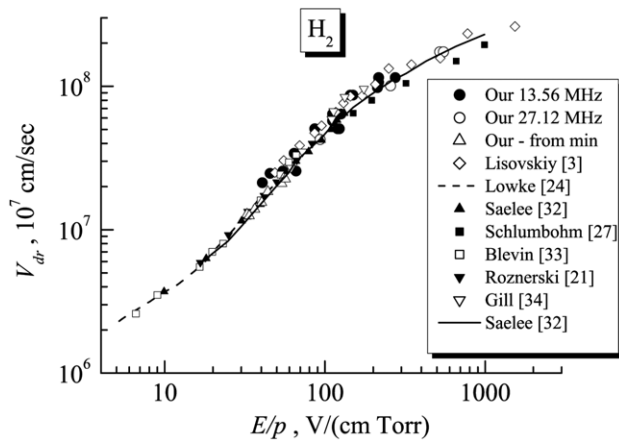


Figure 11. Electron drift velocity in hydrogen against E/p . The solid curve presents the calculated data from [32], the dashed curve presents the calculated data from [24], the solid circles are our experimental data from turning points ($f = 13.56$ MHz), the empty circles are our experimental data from turning points ($f = 27.12$ MHz), the empty upright triangles are our experimental data from minima ($f = 13.56$ MHz and $f = 27.12$ MHz), the empty diamonds are for the experimental data from [3], the solid upright triangles are for the measured data from [32], the solid squares are for the experimental data from [27], the empty squares are for the experimental data from [33], the solid upside-down triangles are for the experimental data from [21] and the empty upside-down triangles are for the experimental data from [34].

velocity over the ranges $E/p = 52\text{--}1324$ $\text{V cm}^{-1} \text{Torr}^{-1}$ for nitrogen, $E/p = 33\text{--}720$ $\text{V cm}^{-1} \text{Torr}^{-1}$ for argon, $E/p = 32\text{--}713$ $\text{V cm}^{-1} \text{Torr}^{-1}$ for ammonia, $E/p = 32\text{--}550$ $\text{V cm}^{-1} \text{Torr}^{-1}$ for hydrogen and $E/p = 69\text{--}1673$ $\text{V cm}^{-1} \text{Torr}^{-1}$ for oxygen. The values of the drift

velocity obtained from our experiments are in good agreement with the previously published data.

Acknowledgments

The authors express their gratitude to the UNAXIS France—Displays division, Palaiseau, France, for their financial support and for the equipment used in this study.

References

- [1] Lisovskiy V A and Yegorenkov V D 1997 *Record-Abstracts IEEE Int. Conf. on Plasma Science (San Diego, USA)* p 137
- [2] Lisovskii V A 1998 *Tech. Phys. Lett.* **24** 308
- [3] Lisovskiy V A and Yegorenkov V D 1998 *J. Phys. D: Appl. Phys.* **31** 3349
- [4] Lisovskiy V A and Yegorenkov V D 1999 *J. Phys. D: Appl. Phys.* **32** 2645
- [5] Lisovskiy V, Martins S, Landry K, Douai D, Booth J-P and Cassagne V 2005 *J. Phys. D: Appl. Phys.* **38** 872
- [6] Levitskii S M 1957 *Sov. Phys.—Tech. Phys.* **2** 887
- [7] Kihara T 1952 *Rev. Mod. Phys.* **24** 45
- [8] Jager G and Otto W 1962 *Z. Phys.* **169** 517
- [9] Kucukarpaci H N and Lucas J 1981 *J. Phys. D: Appl. Phys.* **14** 2001
- [10] Sakai Y, Tagashira H and Sakamoto S 1977 *J. Phys. D: Appl. Phys.* **10** 1035
- [11] Nakamura Y and Kurachi M 1988 *J. Phys. D: Appl. Phys.* **21** 718
- [12] Nielsen R A and Bradbury N E 1937 *Phys. Rev.* **51** 69
- [13] Pack J L, Voshall R E and Phelps A V 1962 *Phys. Rev.* **127** 2084
- [14] Christophorou L G, Carter J G and Maxey D V 1982 *J. Chem. Phys.* **76** 2653
- [15] Ali A W 1988 *Laser Part. Beams* **6** 105
- [16] Nielsen R A and Bradbury N E 1937 *Phys. Rev.* **51** 69
- [17] Naidu M S and Prasad A N 1970 *J. Phys. D: Appl. Phys.* **3** 957
- [18] Jeon B-H and Nakamura Y 1998 *J. Phys. D: Appl. Phys.* **31** 2145
- [19] Brose H L 1925 *Phil. Mag.* **1** 536
- [20] Frommhold L 1964 *Fortschr. Phys.* **12** 597
- [21] Roznerski W and Leja K 1984 *J. Phys. D: Appl. Phys.* **17** 279
- [22] Githens S 1940 *Phys. Rev.* **57** 822
- [23] Chenot M 1948 *Ann. Phys., Paris* **3** 277
- [24] Lowke J J 1963 *Aust. J. Phys.* **16** 115
- [25] Kline L E and Siambis J G 1972 *Phys. Rev. A* **5** 794
- [26] Penetrante B M and Bardsley J N 1984 *J. Phys. D: Appl. Phys.* **17** 1971
- [27] Schlumbohm H 1965 *Z. Phys.* **184** 492
- [28] Wagner E B, Davis F J and Hurst G S 1967 *J. Chem. Phys.* **47** 3138
- [29] Fletcher J and Reid I D 1980 *J. Phys. D: Appl. Phys.* **13** 2275
- [30] Nakamura Y 1987 *J. Phys. D: Appl. Phys.* **20** 933
- [31] Phelps A V and Pitchford L C 1985 *Phys. Rev. A* **31** 2932
- [32] Saelee H T and Lucas J 1977 *J. Phys. D: Appl. Phys.* **10** 343
- [33] Blevin H A, Fletcher J and Hunter S R 1978 *J. Phys. D: Appl. Phys.* **11** 1653
- [34] Gill E B W and von Engel A 1949 *Proc. R. Soc. A* **197** 107